

3D MHD Simulations of Radio Galaxies Including Nonthermal Electron Transport

T. W. Jones & I. L. Tregillis

*School of Physics and Astronomy, University of Minnesota,
Minneapolis, MN, 55455, U.S.A.*

Dongsu Ryu

*Department of Astronomy & Space Science, Chungnam National
University, Daejeon, 305-764, Korea*

Abstract. We report on an effort to study the connections between dynamics in simulated radio galaxy plasma flows and the properties of nonthermal electron populations carried in those flows. To do this we have introduced a new numerical scheme for electron transport that allows a much more detailed look at this problem than has been possible before. Especially when the dynamics is fully three dimensional the flows are generally chaotic in the cocoon, and the jet itself can flail about violently. The bending jet can pinch itself off and redirect itself to enhance its penetration of the ambient medium. These behaviors often eliminate the presence of a strong jet termination shock, which is assumed present in all modern cartoon models of the RG phenomenon. Instead a much more complex “shock web” forms near the end of the jet that leads to a far less predictable pattern of particle acceleration. Similarly, the magnetic fields in these flows are highly filamented, as well as spatially and temporally intermittent. This leads to a very localized and complex pattern of synchrotron aging for relativistic electron populations, which makes it difficult to use properties of the electron spectrum to infer the local rate of aging.

1. Introduction

The interaction between high power plasma jets and the circumgalactic medium (CM) is now the firmly established paradigm for radio galaxies (RGs), as many talks at this meeting verify. The original “twin exhaust” model (Blandford & Rees 1974) outlined how fast plasma jets could possibly carry energy efficiently from the active galactic nucleus (whose nature was still the subject of speculation in 1974) into hot spots of radio lobes, depositing that energy at “working surfaces” associated with the regions where the jets impinged on the ambient medium. Blandford & Rees touched on most of the issues that have occupied researchers in this field over the quarter century since. Those authors perceptively captured a basic concept that seems now clearly to be at the heart of the physics of the radio galaxy phenomenon, and also that previewed discovery of

remarkably similar outflows from an amazing diversity of astrophysical systems. We are still at the task of learning about jet physics more than 25 years later, because the application of the simple concept is actually very complex. Jet-based flows are highly driven systems, inherently unstable and probably always far from any general equilibrium. We still do not properly understand how the jets are formed, what they are made of, how they manage to propagate as much as megaparsecs into the ambient medium, nor how and where the relativistic electron populations we observe in the flows are accelerated nor how they evolve more generally. Those issues, of course, are the central themes of this meeting.

Over the past 15 years or so numerical simulations of time dependent jet flows have progressed enormously from the earliest two dimensional axisymmetric gasdynamical flows (Smith et al. 1985) to three dimensional flows (e.g., Cox, Gull & Scheuer 1991) until now fully three dimensional flows incorporating self-consistent MHD are relatively straightforward, if not yet easy, to model with modest resolution (e.g., Clarke 1997). These simulation methods have also been extended to include flows in either 2D or 3D with relativistic bulk motions (e.g., van Putten 1993; Duncan & Hughes 1994; Aloy et al. 1999; Zhang, Koide & Sakai 1999). Simultaneously, physical models of particle acceleration physics, especially as it relates to the formation of collisionless shocks, have become much better developed (e.g., Jones 2001), even if that cannot yet be called a solved problem. All of these very positive developments have been well represented in presentations at this meeting, in fact.

Most of our information about RGs currently derives from radio synchrotron emissions reflecting the spatial and energy distributions of relativistic electrons convolved with the spatial distribution of magnetic fields. X-ray observations, especially of nonthermal Compton emissions, depending on the electron and ambient photon distributions, are now beginning to add crucial information, as well. Using these connections, much effort has been devoted to interpreting observed brightness, spectral and polarization properties of the nonthermal emissions for estimates of the key physical source properties, such as the energy and pressure distributions and kinetic power, as well as to find self-consistent models for the particle acceleration and flow patterns. As telescopes and analysis techniques have improved the level of detail obtained, it has become apparent, however, that the observed properties are not very simple and much harder to interpret than most simple models predict (e.g., Rudnick 2001).

This problem stems in part from the complexity of the flow dynamics expected, and also for inherent difficulties in simulating both the dynamics and the transport of radiating particles in multi-dimensional flows. The latter is especially challenging. Until now, in fact, all published efforts to model nonthermal emission properties from simulated flow behaviors have been based on ad-hoc simple assumptions about the relationships between nonthermal particles and bulk flow variables such as total fluid pressure, density and magnetic field (e.g., Clarke, Burns & Norman 1989; Matthews & Scheuer 1990; Aloy et al. 2000). To address properly the inherently nonequilibrium character of nonthermal particles, however, it is essential that they be treated explicitly. We report here on our program to do this. It provides the first multi-dimensional numerical simulations of jet-driven flows including acceleration and transport of radiating nonthermal electrons in a fashion that enables detailed study of the connections

between flow dynamics, particle transport and nonthermal emissions. This is made possible by a new and very efficient scheme for nonthermal particle transport (Jones, Ryu & Engel 1999; Jun & Jones 1999). We focus in this paper on the links between plasma dynamics and particle acceleration and transport that we can see with this treatment. A companion paper (Tregillis, Jones & Ryu 2001a) discusses initial “synthetic radio observations” made on our simulated objects. We will see, in fact, that the nonthermal particle and emission properties are often very poorly represented in standard cartoons of RGs.

2. Computational Methods

Flow dynamics in our simulations is treated with a second-order, conservative “TVD” ideal MHD code described in Ryu & Jones 1995, Ryu, Jones & Frank 1995 and Ryu et al. 1998. The method depends on approximate solutions to the 1D MHD Riemann problem at zone boundaries, and uses conventional directional splitting techniques in multiple dimensions to retain second order accuracy. The code maintains the divergence free condition for magnetic fields to machine accuracy using an upwinded constrained transport scheme as described in Ryu et al. 1998. To follow nonthermal particle transport we solve the standard “convection diffusion” equation for the momentum distribution, $f(p)$ (e.g., Skilling 1975). This equation includes the effects of adiabatic and radiative losses as well as terms that account for particle acceleration due to spatial diffusion at shocks and momentum diffusion resulting from MHD turbulence. The computational effort needed to solve this equation over an entire grid is enormous, because it must be solved simultaneously for momenta spanning at least several orders of magnitude, and must capture microphysics taking place on spatial scales also spanning many orders of magnitude. To manage that with conventional finite differencing methods in momentum space would involve vastly more effort than the MHD itself, so is simply not practical. On the other hand, there are a couple of very important properties of the problem that can be utilized to circumvent the difficulties in some circumstances, reducing the work level to being just comparable to the MHD; that is, the total cost and number of variables is about doubled, so manageable.

The first key feature is that $f(p)$ is mostly a smooth and broad function. In fact, away from cutoffs it can be adequately described by defining a “local spectral index”, $q(p) = -\partial \ln f / \partial \ln p$, which varies slowly with p . Thus, we integrate the convection diffusion equation over logarithmic momentum bins at each spatial zone and simply track the number of nonthermal particles in each bin. Those quantities are updated in a conservative scheme using fluxes across momentum boundaries computed from the dynamical variables, magnetic field, radiation field, etc. By applying the simple quasi-power law model for the distribution of $f(p)$ within momentum bins we can make the bins rather large and still maintain good accuracy. For the results shown here we have used eight momentum bins uniformly spread over $\Delta \ln(p) = 12$.

The second key feature is that the microphysics governing $f(p)$ generally takes place on scales within a modest factor of the gyro radii of the particles. For energies of a few tens of GeV and below, relevant to radio synchrotron emission and X-ray Compton emission those length scales and the associated time

scales are at least several orders of magnitude smaller than scales resolved in the MHD solution. Diffusive acceleration up to GeV energies at shocks should be essentially instantaneous on the time scale of RG dynamics, so one can find $f(p)$ immediately behind a shock from the steady state solution there. In the test particle limit that depends only on the shock compression ratio, r , i.e., $q_s = 3r/(r - 1)$, which approaches 4 at strong shocks. Downstream, $f(p)$ becomes modified by adiabatic and radiative effects using the methods outlined in the previous paragraph. This scheme can be implemented to include spatial diffusion, and second order Fermi acceleration, as well as other loss mechanisms. In the present, exploratory simulations, however, we have neglected spatial diffusion, and have included only diffusive shock acceleration, plus adiabatic and radiative losses for nonthermal electrons. We treat the nonthermal electrons as a passive component for now, and have included improvements that enhance the performance of the originally published scheme.

3. Model Dynamics

Jones et al. 1999 carried out several exploratory simulations using these methods for axisymmetric jets. Their purpose, as for us also, was to begin an examination of how best to understand the links between complex RG flow dynamics and nonthermal particle transport properties. They discussed three simulations based on identical flow dynamics, but with different simple idealized models for the nonthermal particle transport properties. Here we discuss extensions of those same three simulations from two to three dimensions. Earlier discussions of some of these results are contained in Jones, Ryu & Tregillis 2000 and Tregillis, Jones & Ryu 2000.

The 3D jets were light ($\rho_j/\rho_a = 10^{-2}$) with an internal Mach number, $M_j = 8$, and assumed to be in pressure balance with a uniform ambient medium (the CM) at their origin. The magnetic field in the in-flowing jet was helical, with a uniform poloidal component, B_{p0} , that mapped into the CM, plus a toroidal component, B_t , derived from a uniform axial current with a return current along the jet boundary. The maximum $B_t/B_{p0} = 2$, while the axial “beta” of the jet plasma was $\beta_0 = 8\pi P_g/B_{p0}^2 = 10^2$. To break axisymmetry the in-flowing jet was made to precess on a 5 degree cone with a period allowing approximately $5\frac{1}{2}$ rotations during the simulation. Thus, our flows have a fully three dimensional flavor very early on. Previous 3D simulations have shown that even numerical perturbations will eventually cause jets to deviate substantially from quasi-2D symmetry (Norman 1996), but only after the jet has propagated many jet radii. On the other hand there is good evidence that at least some jets really do precess (e.g., Condon & Mitchell 1984; Mantovani et al. 1999; Sudou & Taniguchi 2000). The simulations were carried out on a $576 \times 192 \times 192$ grid with open boundary conditions except for the jet origin. The in-flowing jet had a top hat velocity profile inside a radius of 15 zones, with a thin sheath around it. Thus, the long dimension of the computational domain was approximately 38 jet radii. These flows are, therefore, still relatively “young” compared to most RGs. Our initial objectives depend on maintaining a reasonably fine resolution of the dynamical structures in the jets and their “heads”, so the large effort needed in these simulations constrains us to look at young flows for the moment.

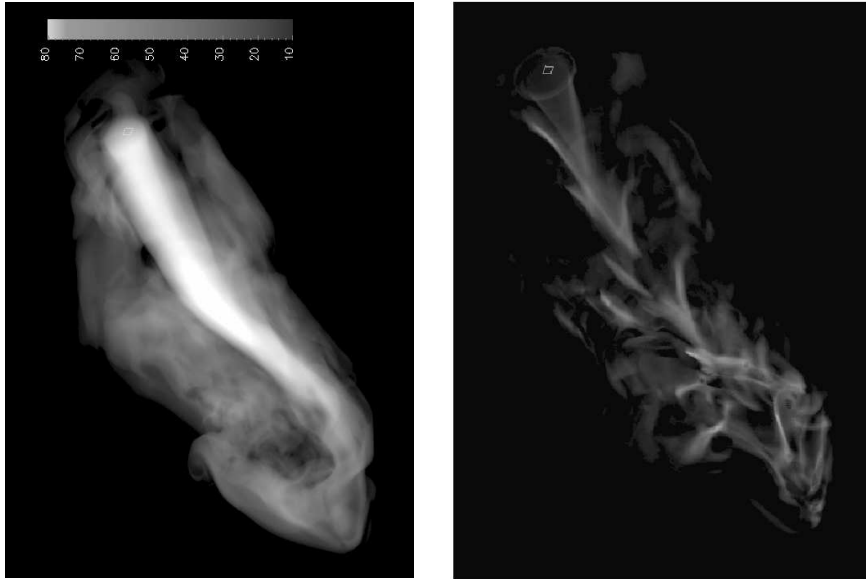


Figure 1. Left: Volume rendering of the flow speed in a Mach 8 MHD jet and its cocoon. The jet has penetrated the CM a little over 30 jet radii at this time. Only plasma entering the grid through the jet is rendered visible here and in all the other figures, as well. Right: Shock structures accompanying the flow shown.

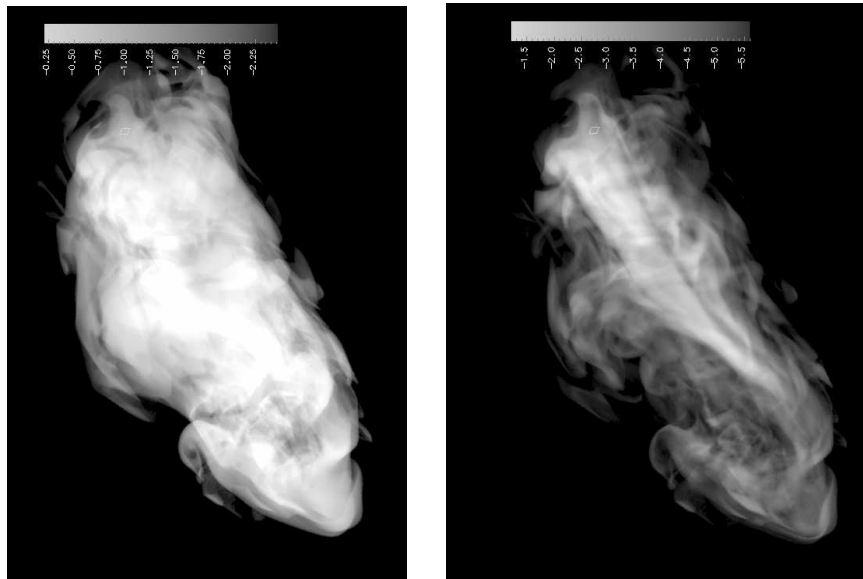


Figure 2. Left: Volume rendering of the log of the gas pressure. Right: The distribution of log of the magnetic pressure.

Figures 1 and 2 illustrate some of the basic dynamical properties of the simulated flows about 90% of the way to the end time. All of the images shown here are volume renderings filtered to show only plasma that entered the grid through the jet origin. That is, we have used a passive mass fraction variable and made transparent any zone containing less than 99% jet material by mass. Figure 1 represents the velocity field in this manner. The left panel displays the flow speed of the jet and its cocoon. The jet itself is clear, of course, but note also that flow speeds in the cocoon can be a substantial fraction of the jet speed. It is also obvious that the cocoon flow is not regular at all. That point is made more dramatic in the right panel of Figure 1, which displays flow compression; i.e., $\nabla \cdot u$. The image isolates shocks in the flow. While such classic features as conical shocks near the jet origin are evident, it is hard to identify anything resembling the canonical “jet termination shock”. Rather, the head of the flow is filled with a “shock web”, and most of it involves back flows in the cocoon rather than the jet itself. There is a very small jet termination shock near the bottom right of the image, but close examination shows that very little of the jet flow actually passes through it.

We have produced several animations, including flow speed, flow compression and magnetic pressure for the entire simulation in order to study the flow properties and to explain the features seen here. Those are currently available for viewing at URL

<http://www.msi.umn.edu:80/Projects/twj/radjet/radjet.html>. Almost as soon as the jet terminus propagates past the position of the first conical shock all semblance of any simple symmetry vanishes. The end of the jet begins to “flail” violently, occasionally isolating pieces of initially high speed plasma that dissipate or run into the wall of the cocoon. The main jet flow then extends forward abruptly, sometimes seeming to poke a sharp “finger” into the CM. These structures resemble hybrids of the so-called “dentist’s drill” (Scheuer 1982) and “splatter spot” (Lonsdale & Barthel 1986) concepts for production of secondary hotspots, and confirm behaviors seen in some earlier 3D simulations (Cox, Gull & Scheuer 1991). Most of the time there is no recognizable jet termination shock, but the violence of the end of the jet flow maintains a complex shock web similar to that visible in Figure 1. Most of the shock surfaces are relatively weak compared to what one would derive for the 1D jet termination shock (the latter strength being for a light jet roughly the jet internal Mach number). Some portions of the shock web can, however, equal or exceed that strength. Generally speaking flows within the cocoon in this simulation are backwards directed, but also highly chaotic, as the shock web indicates.

Figure 2 illustrates the distribution of the log of gas pressure, P_g and magnetic pressure, P_b , for the same time as in Figure 1. Note first that there is considerable intermittency to both distributions. For P_g this reflects the complex flows within the cocoon, since cocoon shocks will enhance P_g and pressure gradients drive the chaotic motions, as well. There is very little similarity in the details of the distributions of P_g and P_b , however. The strongest magnetic fields are generated primarily by flow shear, not compression, so this is expected. The filamentary nature of the magnetic field is evident in the image, and it is clear that the magnetic pressure is much more intermittent than the gas pressure, as we would expect in a system that is this strongly driven and so far from equilibrium. Local variations in P_b of two orders of magnitude are typical, with

much larger excursions into occasional magnetic voids. Peak field strengths in the cocoon are comparable to the jet field, but the average cocoon field generally is much less on account of rarefaction in flows emerging from the jet. We cannot say, of course, how the magnetic field would evolve on scales smaller than our numerical resolution, but on our grid the magnetic field never approaches equipartition with the thermal plasma; i.e., $\beta \gg 1$ everywhere. There are times and places where $M_A = (4\pi u\sqrt{\rho})/|B| < 1$, however, so that magnetic stresses exceed Reynolds stresses. The magnetic field is not entirely passive, in other words, even though on average it would appear so. We note also that the animation of the magnetic pressure reveals brief episodes when the peak field strength near the jet terminus is considerably stronger than average. Those episodes correspond to times when the jet extends itself most rapidly into the CM as it “breaks” and reforms.

In summary, the terminus of our light 3D jet behaves in a violently unstable manner that makes the concept of a simple jet termination shock not very applicable, while creating a chaotic cocoon with a rich web of shocks and highly filamentary, intermittent magnetic fields.

4. Nonthermal Electron Acceleration and Transport

On top of the dynamics just described we computed the evolution of nonthermal electron populations using the methods outlined in §2. We emphasize that our purpose at this stage of the program is not to look for the parameters that necessarily most resemble real RGs, but, rather to understand how particle populations will behave under simple assumptions and how “synthetic observations” of the simulated objects behave. Further, we want to know and what that tells us that we can reliably derive from observations when we know the actual source physical properties.

We simulated three models for nonthermal electron transport analogous to those discussed by Jones et al. 1999 for similar, but axisymmetric flows. In all three models nonthermal electrons passing through shocks are accelerated according to standard test particle diffusive shock acceleration theory (e.g., Drury 1983), so that a momentum distribution becomes flattened to $f(p) \propto p^{-q_s}$, if initially steeper, where $q_s = 3r/(r-1)$, and r is the shock compression ratio. In all three models electrons in smooth flows are subject to adiabatic energy gains and losses as a result of flow expansion or compression.

In two of the models all the nonthermal electrons are introduced only at the jet origin, whence they are advected with the jet plasma. Those electron populations enter with a power law momentum distribution, $f(p) \propto p^{-q_j}$, with $q_j = 4.4$, which corresponds to a synchrotron spectral index $\alpha = 0.5(q-3) = 0.7$, typical for jets. These two models differ only in the rates of radiative cooling for the nonthermal electrons. In our “control model”, radiative cooling is negligible, whereas in the “strong-cooling model” an electron with momentum $\hat{p} = 10^4 mc$ ($E = 5$ GeV) would lose half its initial energy to synchrotron radiation in a field B_{p0} over the full duration of the simulation. For the parameters used to create synthetic observations (Tregillis et al. 2001a) we used $B_{p0} = 5.8\mu G$. In that field such electrons would radiate synchrotron emission near 2.4 GHz and their radiative lifetimes would be about 50 million years, thus defining the

duration of the simulation. We note that since the equations of ideal MHD have no inherent time or length scales, the dynamics can be computed without any reference to physical units. Defining radiative cooling rates constrains physical parameters, but, as discussed in Jones et al. 1999, it is still possible to rescale the physical system in order to keep the dynamics unchanged while adjusting the electron cooling rates. That is what we have done here. The intent is to explore how electron “aging” takes place in the simulated flows, taking into account the highly intermittent character of the magnetic fields.

The third electron transport model injects new nonthermal electrons from the thermal plasma at shocks and then follows them in a manner analogous to the control model. Evidence from galactic shocks, such as supernova remnants, strongly suggests that a fraction of the thermal electron population passing through a collisionless shock is injected into the nonthermal population, although the physics of that process is still unclear (e.g., Jones 2001). Here we apply a simple injection model that extracts a small, fixed fraction (10^{-4}) of the total electron flux through a shock. The intent of the “injection model” simulation is to examine the effects of the complex shock web on particle spectra when the population is dominated by in situ injection. Thus, radiative cooling is made negligible and the nonthermal electron population entering at the jet origin is small, as well.

The electron spectral distributions of all three transport models are intricate, reflecting the complex shock and magnetic field properties discussed earlier. The chaotic motions in the cocoon make it difficult to identify the immediate causes of any particular feature in a local electron population. Generally speaking, the local particle spectra usually depend more directly on where the particles have been than what their current local environment is like. In a complex, changing flow, that is difficult to reconstruct that history from snapshots.

We offer a few comments on the individual model behaviors, but for details refer readers to a more complete discussion in preparation (Tregillis, Jones & Ryu 2001b). For the control model the entire electron population has spectra flatter than $q_j = 4.4$, since diffusive shock acceleration can only flatten the spectrum. From standard relations one can easily compute the minimum shock strength necessary to flatten an incident electron population; namely, $M = \sqrt{q_s/(q_s - 4)}$ (with $\gamma = \frac{5}{3}$). Shock modification of the electron population entering with the jet requires passage through shocks of modest strength; namely, $M > 3.3$. However, just as in the earlier axisymmetric results, there is little evidence of particle acceleration directly associated with a dominant jet terminal shock. Too little of the jet flow exits through such a shock structure to have a global impact. Instead, the evident particle acceleration is associated with strong shock sites within the shock web near the jet terminus. Those tend to vary quickly over both space and time. Thus, the particle spectral distribution shows much delicate structure, which is difficult to capture in gray scale, but which is evident in the color image given in Jones et al. 2000 and on the previously mentioned web site.

The effect of the shock web is easily apparent in the electron spectral distributions shown for the injection model in the left panel of Figure 3. The images in this figure come from the same time as those in Figures 1 and 2, and the orientation of the grid is the same, as well. They render the spatial distribution

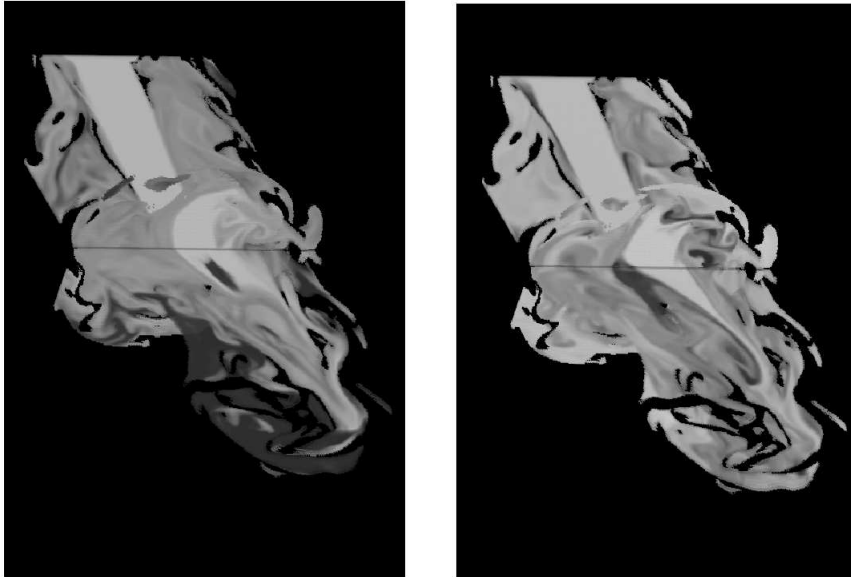


Figure 3. Pairs of orthogonal slices through the grid rendering the spectral index of 5 GeV electrons. Left: The “injection” model, in which the electron population is dominated by fresh injection at shocks in the flow. Radiative cooling is negligible. Right: The “strong cooling” model, in which 5 GeV electrons just cool over the duration of the simulation if embedded in the nominal jet magnetic field. High tones represent flatter spectra.

of q for 5 GeV electrons, with flatter spectra having higher tones. The image is not weighted by emissivity, so cannot alone tell us the expected synchrotron spectrum along a given line of sight. That property requires a radiative transfer calculation based on self-consistent emissivities, which is done in the companion paper by Tregillis et al. 2001a. To view $q(5\text{GeV})$ we have taken a 2D slice down the center of the computational box and a transverse one as well. Again only plasma that is entirely of jet origin is rendered. The remaining space is transparent. As an aside we note that the irregular boundary of the visible regions emphasizes the fact that some large scale mechanical mixing is taking place between the jet cocoon and the CM in response to Kelvin-Helmholtz instabilities.

The jet can be seen entering from the top. A very small population of nonthermal electrons is actually introduced by the in-flowing jet with $q = q_j = 4.4$ in this model, making the jet visible here. Almost everywhere else, the electron population is completely dominated by injection at the shocks within the flow, however. Mostly the electron spectral slope lies in the range $4.4 < q < 5.5$, but there are pockets of larger and smaller values, as well. We see for these slices that most of the volume is occupied by electron populations with spectra moderately steeper than q_j for the incoming jet. That reflects the fact that most of the plasma gets processed only by relatively weak shocks, as we discussed earlier. Sometimes a particular slope value streams into the back-flow, identifying relatively long lived shock structures and their downstream flow patterns. This is about the closest the patterns come to the canonical model in which all the cocoon flow represents flow after passage through a unique,

strong jet termination shock. The more realistic situation is clearly much more complicated.

The right panel in Figure 3 shows the analogous electron spectral index distribution in the “strong cooling” transport model. Recall in this model that all the nonthermal electrons entered with the jet, so the only role of shocks is to flatten portions of the momentum spectrum steeper than q_s as a population enters the shock. Thus, without radiative cooling all rendered regions in this image would show tones (“brightness”) at least as high as the in-flowing jet. For this model, 5 GeV electrons would just cool over the duration of the simulation if they sat in a magnetic field equal to the jet poloidal value, B_{p0} . Of course, electrons actually spend a much shorter time inside the jet itself, since jet plasma would cross the computational grid in about $\frac{1}{10}$ the simulation time if it were not deflected by the ambient medium along the way. So, there is little “aging” of the electron population at this energy within the jet flow. The most notable property of the distribution outside the jet is its complex structure showing that spectral aging is not a smooth function of location, and certainly not a simple measure of distance from the jet terminus. In fact one can again identify “streams” of nearly constant q that roughly correspond to the patterns of flow. Mostly $4.4 < q < 5$, but both flatter and steeper pockets are scattered through the volume. Thus, most of the cocoon electron population has experienced some amount of radiative cooling at this energy, as intended for this model. On the other hand that cooling has mostly taken place very near the head of the flow, and it is not uniform. That pattern is quite consistent, in fact, with the properties of the magnetic field as illustrated in Figure 2, especially when one accounts for the episodes of stronger field amplification mentioned in the dynamical discussion. From these behaviors it is clearly very risky to attempt to use synchrotron spectral distributions to infer local spectral aging rates.

5. Conclusions

We have begun an effort to study the connections between dynamics in simulated radio galaxy plasma flows and the properties of nonthermal electron populations carried in those flows. To do this we have introduced a new numerical scheme for electron transport that allows us a much more detailed look at this problem than has been possible before. Especially when the dynamics is fully three dimensional the flows are generally chaotic in the cocoon, and the jet itself can flail about violently. The deflected jet can pinch itself off and redirect itself to enhance its penetration of the ambient medium. These behaviors mostly eliminate the presence of a strong jet termination shock, which is assumed present in all modern cartoon models of the RG phenomenon. Instead a much more complex “shock web” forms near the end of the jet that leads to a far less predictable pattern of particle acceleration. Similarly, the magnetic fields in these flows are highly filamented, as well as spatially and temporally intermittent. This leads to a very localized and complex pattern of synchrotron aging for relativistic electron populations, which makes it difficult to use properties of the electron spectrum to infer the local rate of aging.

These results may appear discouraging to interpretation of observations at first glance, but we aim through this study to establish a more robust physical

basis for linking observed source properties with physical model characteristics, and so to define firmly such key properties as the power of the jets that drive these phenomena. An important step in that task is the use of synthetic observations of the simulated objects. That effort is also underway as described in our companion paper in these proceedings (Tregillis et al. 2001a).

Acknowledgments. Work by TWJ and ILT has been supported under NSF grants AST96-16964 and AST00-71167, as well as the University of Minnesota Supercomputing Institute. Work by DR has been supported by KOSEF grant KRF-2000-015-DS0046.

References

- Aloy, M.-A., Gómez, J., Ibáñez, J., Martí & Müller, E. 2000, ‘Radio Emission from Three-dimensional Relativistic Hydrodynamic Jets: Observational Evidence of Jet Stratification’, *ApJ*, 528, L85-L88
- Blandford, R. D. & Rees, M. J. 1974, ‘A Twin Exhaust Model for Double Radio Sources’, *Nature*, 169, 395-415
- Clarke, D. 1997, ‘A Restarting Jet Revisited: MHD Computations in 3-D’ in *Computational Astrophysics; 12th Kingston Meeting on Theoretical Astrophysics; ASP Conference Series #123*, edited by D. A. Clarke and M. J. West., p. 255
- Clarke, D., Burns, J. & Norman, M. 1989, ‘Numerical observations of a simulated jet with a passive helical magnetic field’, *ApJ*, 342, 700-717
- Condon, J. J. & Mitchell, K. J. 1984, ‘4C 29.47 - Quasi-periodic outbursts recorded by precessing jets?’, *ApJ*, 276, 472-475
- Cox, C., Gull, S. & Scheuer, P. 1991, ‘Three-dimensional simulations of the jets of extragalactic radio sources’, *MNRAS*, 252, 558-585
- Drury, L. O’C. 1983, ‘An Introduction to the theory of diffusive shock acceleration of energetic particles in tenuous plasmas’, *Rep. Prog. Phys.*, 46, 973-1027
- Duncan, G. & Hughes, P. 1994, ‘Simulations of relativistic extragalactic jets’, *ApJ*, 436, L119-L122
- Jones, T. W. 2001, ‘Cosmic Particle Acceleration: Basic Issues’, in *7th Taipei Astrophysics Workshop on Cosmic Rays in the Universe’ ASP Conf. Series*, in preparation
- Jones, T., Ryu, D. & Engel, A. 1999, ‘Simulating Electron Transport and Synchrotron Emission in Radio Galaxies: Shock Acceleration and Synchrotron Aging in Axisymmetric Flows’, *ApJ*, 512, 105-124
- Jones, T., Tregillis & Ryu, D. 2000, ‘Simulations of Nonthermal Electron Transport in Multidimensional Flows: Application to Radio Galaxies’, in *Life Cycles of Radio Galaxies, New Astronomy Reviews (Elsevier Science)*, edited by J. Biretta (in press).
- Jun, B. & Jones, T. 1999, ‘Radio Emission from a Young Supernova Remnant Interacting with an Interstellar Cloud: Magnetohydrodynamic Simulation with Relativistic Electrons’, *ApJ*, 511, 774-791

- Lonsdale, C. & Barthel P. 1986, 'Double hotspots and flow redirection in the lobes of powerful extragalactic radio sources', *AJ*, 92, 12-22
- Matthews, A. & Scheuer, P. 1990, 'Models of radio galaxies with tangled magnetic fields. I - Calculation of magnetic field transport, Stokes parameters and synchrotron losses. II - Numerical simulations and their interpretation', *MNRAS*, 242, 616-635
- Mantovani, F., Junor, W. Valero, C. & McHardy, I 1999, 'VLBI observations of 3C 273 at 22 GHz and 43 GHz. I. Search for short time-scale structural variation', *ã*, 346, 397-406
- Norman, M. 1996, 'Structure and Dynamics of the 3D Supersonic Jet', in *Energy transport in radio galaxies and quasars*, ASP Conf. Series 100, ed. P. Hardee, A. Bridle & J. Zensus, p 319
- Rudnick, L. 2001, 'What Shape are Your Spectra In?', this volume
- Ryu, D. & Jones, T. 1995, 'Numerical magnetohydrodynamics in astrophysics: Algorithm and tests for one-dimensional flow', *ApJ*, 442, 228-258
- Ryu, D., Jones, T. & Frank, A. 1995, 'Numerical Magnetohydrodynamics in Astrophysics: Algorithm and Tests for Multidimensional Flow', *ApJ*, 452, 785-796
- Ryu, D., Miniati, F., Jones, T. & Frank, A. 1998, 'A Divergence-free Upwind Code for Multidimensional Magnetohydrodynamic Flows', *ApJ*, 509, 244-255
- Scheuer, P. 1982, 'Morphology and power of radio sources', in *Extragalactic radio sources (Dordrecht)* p 163-165
- Skilling, J. 1975, 'Cosmic ray streaming. I - Effect of Alfvén waves on particles', *MNRAS*, 172, 557-566
- Smith, M., Norman, M., Winkler, K. & Smarr, L. 1985, 'Hotspots in radio galaxies - A comparison with hydrodynamic simulations', *MNRAS*, 214, 67-85
- Sudou, H. & Taniguchi, Y. 2000, 'Large-Scale Regular Morphological Patterns in the Radio Jet of NGC6251', *AJ*, 120, 697-702
- Tregillis, I., Jones, T., Ryu, D. & Park, C. 2000, 'Simulations of Nonthermal Electron Transport in Multidimensional Flows: Synthetic Observations of Radio Galaxies', in *Life Cycles of Radio Galaxies*, *New Astronomy Reviews (Elsevier Science)*, edited by J. Biretta (in press)
- Tregillis, I., Jones & Ryu 2001a, 'Nonthermal Emissions in Radio Galaxies from Simulated Relativistic Electron Transport in 3D MHD Flows', this proceedings
- Tregillis, I., Jones, T. & Ryu, D. 2001b, '3D MHD Simulations of Relativistic Electron Transport and Nonthermal Emission in Radio Galaxies', *ApJ*(to be submitted)
- van Putten, M. 1993, 'A two-dimensional relativistic ($\Gamma = 3.25$) jet simulation', *ApJ*, 408, L21-L23
- Zhang, H., Koide, S. & Sakai, J. 1999, 'Two-Dimensional Simulations of Relativistic Jet-Cloud Collisions', *PASJ*, 51, 221-231